Human $G_{s\alpha}$ mutant causes pseudohypoparathyroidism type Ia/neonatal diarrhea, a potential cell-specific role of the palmitoylation cycle

Noriko Makita*, Junichiro Sato*, Philippe Rondard†, Hiroshi Fukamachi‡, Yasuhito Yuasa‡, Micheala A. Aldred§, Makiko Hashimoto*, Toshiro Fujita*, and Taroh Iiri*¶

*Department of Endocrinology and Nephrology, University of Tokyo School of Medicine, 7-3-1, Hongo, Bunkyo-ku, Tokyo 113-8655, Japan; †Institut de Génomique Fonctionnelle, 141 Rue de la Cardonille, 34094 Montpellier Cedex 5, France; ‡Department of Molecular Oncology, Graduate School of Medicine and Dentistry, Tokyo Medical and Dental University, 1-5-45 Yushima, Bunkyo-ku, Tokyo 113-8549, Japan; and §Division of Medical Genetics, University of Leicester and Leicestershire Genetics Service, University Hospitals of Leicester NHS Trust, Leicester, United Kingdom

Communicated by Henry R. Bourne, University of California, San Francisco, CA, September 19, 2007 (received for review June 1, 2007)

Pseudohypoparathyroidism type Ia (PHP-Ia) results from the loss of one allele of $G_{s\alpha}$, causing resistance to parathyroid hormone and other hormones that transduce signals via G_s. Most $G_{s\alpha}$mutations cause the complete loss of protein expression, but some cause loss of function only, and these have provided valuable insights into the normal function of G proteins. Here we have analyzed a mutant $G_{s\alpha}$ (αs-AVDT) harboring AVDT amino acid repeats within its GDP/GTP binding site, which was identified in unique patients with PHP-Ia accompanied by neonatal diarrhea. Biochemical and intact cell analyses showed that αs-AVDT is unstable but constitutively active as a result of rapid GDP release and reduced GTP hydrolysis. This instability underlies the PHP-Ia phenotype. αs-AVDT is predominantly localized in the cytosol, but in rat and mouse small intestine epithelial cells (IEC-6 and DIF-12 cells) αs-AVDT was found to be localized predominantly in the membrane where adenylyl cyclase is present and constitutive increases in cAMP accumulation occur in parallel. The likely cause of this membrane localization is the inhibition of an activation-dependent decrease in αs palmitoylation. Upon the overexpression of acyl-protein thioesterase 1, however, αs-AVDT translocates from the membrane to the cytosol, and the constitutive accumulation of cAMP becomes attenuated. These results suggest that PHP-Ia results from the instability of αs-AVDT and that the accompanying neonatal diarrhea may result from its enhanced constitutive activity in the intestine. Hence, palmitoylation may control the activity and localization of $G_{s\alpha}$ in a cell-specific manner.

disease | G protein | lipid modification | localization | activity

G protein diseases have revealed key pathways underlying physiologic regulation and the molecular mechanisms involved. Pseudohypoparathyroidism type Ia (PHP-Ia) is a classic example of such a disease and results from the heterozygous loss of function of $G_{s\alpha}$ (1–4). In most cases, the loss of $G_{s\alpha}$ function results from a loss of protein expression due to insertions, deletions, frameshift deletions, nonsense mutations, and splice junction mutations. In some cases, however, PHP-Ia occurs in the presence of $G_{s\alpha}$ protein expression, and analyses of the corresponding mutations have greatly furthered our understanding of how G proteins function normally (5).

The activity of $G_{s\alpha}$ is cyclically regulated via two unidirectional steps, a GDP/GTP exchange and the hydrolysis of GTP (5–8). The agonist-occupied receptor accelerates GDP release from the $\alpha\beta\gamma$ trimer, which allows GTP to bind to the empty guanine nucleotide pocket of G_α and thus induce a conformational change that enables its dissociation from the receptor and $\beta\gamma$ subunit. The GTP-bound G_α and $\beta\gamma$ dimer transmit a signal until GTP is hydrolyzed, which then allows the GDP-bound G_α to bind and inactivate $G_{\beta\gamma}$.

The defects resulting from $G_{s\alpha}$ mutations that do not prevent protein expression but nevertheless result in the onset of PHP-Ia have now been elucidated at the molecular level and have provided invaluable information regarding how G proteins operate in this G_α cycle. The αs-R386H (9) and αs-Y391X (10, 11) mutations result in a loss of $G_{s\alpha}$ function by preventing receptor interactions. The αs-A366S defect shows not only a loss of function resulting from rapid denaturation of the $G_{s\alpha}$ protein but also a gain of function resulting from its relative stabilization at 33°C (12). Additional loss-of-function $G_{s\alpha}$ mutations include αs-R231H, which confers a conditionally defective activation (13, 14), and αs-R280K, which may be defective in G protein–effector interactions (10). Moreover, some missense $G_{s\alpha}$ mutants (S250R and R258W), which are not expressed in human cells but can be generated by *in vitro* translation, have also contributed to our understanding of the kinetics of GTPase in the G_α cycle (15, 16).

To identify instructive $G_{s\alpha}$ mutants, we predicted that it would be useful to investigate atypical PHP-Ia patients who show (*i*) a classic PHP-Ia phenotype and normal protein expression or (*ii*) a phenotype other than the classic PHP-Ia phenotype. Such mutants would be expected to provide further data regarding the functions of G proteins. Here we have analyzed a unique case of familial PHP-Ia accompanied by neonatal diarrhea and identified a mutant $G_{s\alpha}$ harboring AVDT amino acid repeats within its $\beta6/\alpha5$ loop (Fig. 1). This loop is responsible for the interaction of the G protein with the guanine ring of GDP/GTP (17). Two sibling patients, a female and a male, showed a PHP-Ia phenotype including hypocalcemia, resistance to parathyroid hormone, and increased levels of thyroid-stimulating hormone. In addition, both of these patients uniquely presented with neonatal diarrhea, which was transient and corrected itself spontaneously after several months, suggesting that this phenotype may also result from the AVDT mutant $G_{s\alpha}$ (17). Here we have analyzed this mutant to clarify the molecular mechanisms underlying the onset of PHP-Ia/neonatal diarrhea.

Results

The AVDT Mutant Is Constitutively Active but Unstable. To characterize the αs-AVDT mutant G protein, we purified both recombinant αs-AVDT and αs-WT from the cytosol of Sf9 cells by using a baculovirus system (see *Materials and Methods* for details). We then used these preparations in a guanosine 5′-[γ-thio]triphosphate (GTP[γS]) binding assay, and found that the apparent "on" rate of GTP[γS] (k_{app}) was 30-fold higher for

Author contributions: N.M. and J.S. contributed equally to this work; N.M. and T.I. designed research; N.M., J.S., P.R., H.F., M.A.A., M.H., and T.I. performed research; N.M., Y.Y., T.F., and T.I. analyzed data; and N.M. and T.I. wrote the paper.

The authors declare no conflict of interest.

Abbreviation: PHP-Ia, pseudohypoparathyroidism type Ia.

¶To whom correspondence should be addressed. E-mail: tiiri-tky@umin.ac.jp.

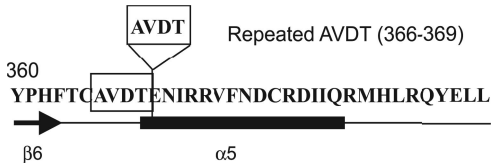

Fig. 1. Carboxyl-terminal sequence of αs-AVDT. The AVDT (366–369) amino acid moiety that is present as a repeat sequence in the αs-AVDT mutant is boxed.

αs-AVDT (7 min^{-1}) than for αs-WT (0.22 min^{-1}) (Fig. 2*A*). In a steady-state GTPase assay, we further found that the steady-state GTPase rate (k_{ss}) for αs-AVDT was 0.9 min^{-1}, compared with a rate of 0.22 min^{-1} for αs-WT (Fig. 2*B*). Moreover, the rate constant for a single turnover of GTP hydrolysis (k_{cat}) for αs-AVDT was calculated to be ≈1 min^{-1} based on the following approximation: $1/k_{ss} \approx 1/k_{app} + 1/k_{cat}$ (18). That of αs-WT, however, was measured at 3.4 min^{-1} (data not shown). These data indicate that in the presence of GTP, the rate-limiting step in the G_α cycle of αs-WT is the release of GDP as reported earlier, whereas in the case of αs-AVDT this rate-limiting step is the hydrolysis of GTP.

These results suggest that, compared with αs-WT, αs-AVDT has two distinct characteristics in the αs cycle: a rapid GDP release and a slightly reduced rate of GTP hydrolysis. Hence, in the presence of GTP, which is the major guanine nucleotide in the cells, αs-AVDT should predominate in its GTP-bound form and be capable of activating adenylyl cyclase without receptor stimulation, resulting in its constitutive activation. To confirm that this is the case, we added recombinant αs-WT or αs-AVDT to the membranes of S49 cyc^- lymphoma cells, which lack endogenous αs, in the presence of various guanine nucleotides. In the presence of GTP[γS] or AlF_4^-, both αs-WT and αs-AVDT activated the adenylyl cyclase of the cyc^- membranes equivalently (Fig. 2 *C* and *D*). When guanosine 5′-[β-thio]diphosphate (GDP[βS]) was used, neither αs-WT nor αs-AVDT promoted cAMP production. Significantly, however, with GTP, αs-AVDT activated adenylyl cyclase to the same extent as it did in the presence of GTP[γS], whereas αs-WT did not show any activation. These results indicate that αs-AVDT is indeed constitutively active in the presence of GTP as predicted (Fig. 2*D*).

In its guanine nucleotide-free form, αs denatures more rapidly than in its GDP/GTP bound form (12). Given that αs-AVDT harbors large mutations within its GDP/GTP binding site, we speculated whether this mutant G protein might be impaired in GDP/GTP binding, leading to an inherent instability (see also *Discussion*). To test this possibility biochemically, we incubated αs-WT and αs-AVDT with GTP[γS] or GTP and measured the remaining levels of each protein by testing its ability to stimulate adenylyl cyclase in the membranes of cyc^- cells or to bind radioactive GTP[γS]. When incubated with GTP[γS], both αs-AVDT and αs-WT were found to be stable. In contrast, when incubated with GTP, αs-AVDT showed an ≈60-fold more rapid denaturation at 22°C compared with αs-WT, indicating that this

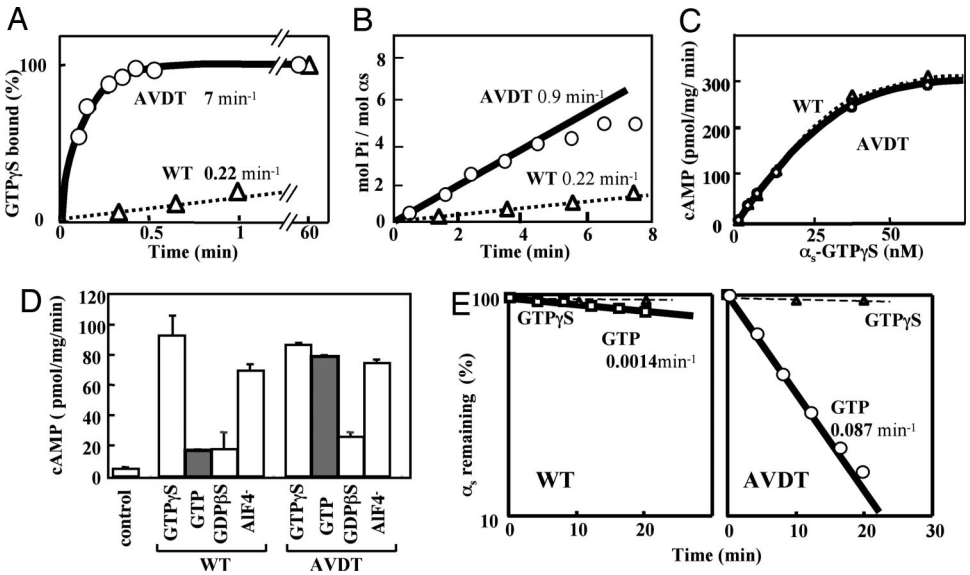

Fig. 2. Biochemical properties of recombinant WT (αs-WT) and mutant (αs-AVDT) αs proteins. (*A*) Rates of GTP[γS] binding. Recombinant αs-WT (triangles) and αs-AVDT (circles) proteins (each at 40 nM) were incubated at 22°C with 1 μM [^{35}S]GTP[γS] (2.2×10^5 cpm/pmol) in buffer A [20 mM Na-Hepes, pH 7.4/10 mM $MgSO_4$/0.1 mM EDTA/3 mM 2-mercaptoethanol/0.025% polyoxyethylene (10) lauryl ether ($C_{12}E_{10}$)]. At the times indicated, the reaction was terminated, and GTP[γS] binding was quantitated by filtration on nitrocellulose membranes. The apparent on rates of GTP[γS] binding (k_{app}) were then calculated by fitting the data to the equation $B = B_{eq}(1 - e^{-kt})$ as described in *Materials and Methods*, where *B* is the concentration of bound GTP[γS], B_{eq} is the equilibreated concentration of binding sites, *k* is the constant describing the rate of approach of the reaction to B_{eq}, and *t* is time. (*B*) Steady-state GTPase. Forty nanomolar of recombinant αs-WT (triangles) or αs-AVDT (circles) was incubated for the indicated times at 22°C with 2 μM [γ-^{32}P]GTP (2×10^5 cpm/$pmol^{-1}$) in buffer A. At the times indicated, the reactions were terminated, and phosphate release was quantified by charcoal adsorption. The steady-state GTPase rates (k_{ss}) were then calculated. Pi, inorganic phosphate. (*C*) cAMP synthesis stimulated by different concentrations of αs-WT or αs-AVDT in the presence of GTP[γS]. Reactions were performed at 20°C for 10 min in 75-μl volumes containing 22.5 μg of cyc^- cell membranes, as described previously (12, 47) apart from minor changes to the buffer conditions. These included 50 mM Na-Hepes (pH 7.4), 6 mM $MgCl_2$, 0.01% $C_{12}E_{10}$, and 50 μg ml^{-1} BSA. Before the assay, the αs proteins were incubated with 100 μM GTP[γS] for 30 min (αs-WT) or 1 min (αs-AVDT). (*D*) The effects of the indicated different guanine nucleotides on cAMP synthesis in the presence of 15 nM αs-WT or αs-AVDT. Reactions were conducted at 20°C for 10 min as described in *C*. Before the assay commenced, the αs proteins were incubated with GTP[γS], GTP, or guanosine 5′-[β-thio]diphosphate (GDP[βS]), each at 100 μM, or with 20 μM $AlCl_3$ and 10 mM NaF for 30 min (αs-WT) or 1 min (αs-AVDT). (*E*) The protein stability of αs-WT or αs-AVDT assessed *in vitro* by [^{35}S]GTP[γS] binding. Recombinant αs-WT or αs-AVDT (each at 30 nM) was incubated at 22°C with the indicated concentrations of GTP or GTP[γS]. At the times indicated, 5-μl aliquots were withdrawn and assayed for GTP[γS] binding in 20-μl reaction mixtures. The values represent the means ± SD of triplicate determinations, and each set of results is representative of at least two additional experiments.

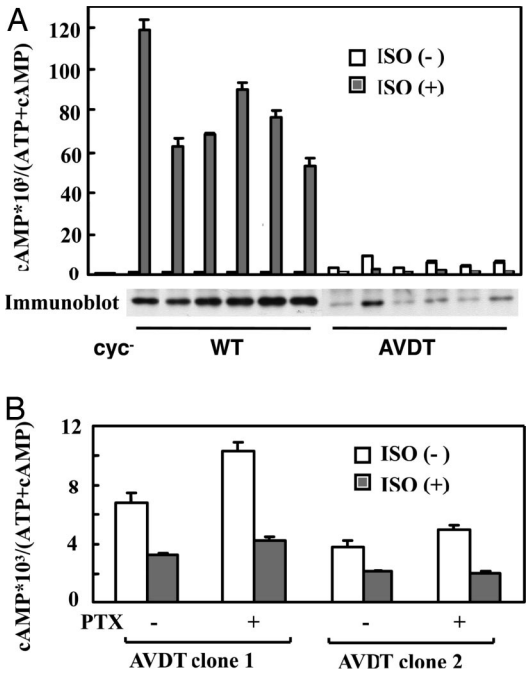

Fig. 3. cAMP accumulation and the expression of recombinant αs proteins in S49 cyc⁻ stable clones expressing HA-tagged αs-WT or HA-tagged αs-AVDT. (*A*) For each transfected cyc⁻ cell clone, the open bars and filled bars indicate the cAMP accumulation levels after 30 min in cells without or with 10 μM isoproterenol, respectively (see *Materials and Methods*). (*Lower*) For immunoblotting analysis, proteins from these clones were detected by using the monoclonal antibody 12CA5 directed against the HA tag, after immunoprecipitation with the same antibody. (*B*) Two stable cyc⁻ clones expressing αs-AVDT were incubated without or with 200 ng/ml pertussis toxin (PTX) for 12 h. cAMP accumulation without or with 10 μM isoproterenol was then assayed as described in the *Materials and Methods*. The values shown in these analyses represent the means ± SD of triplicate determinations. Each set of results is representative of at least two additional experiments.

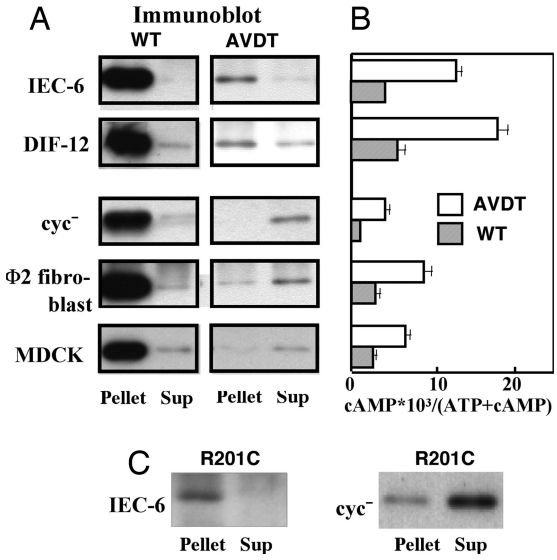

Fig. 4. Localization of recombinant αs proteins and measurement of cAMP accumulation. (*A*) The localization of recombinant αs proteins in cells stably expressing αs-WT or αs-AVDT. IEC-6 (2.0×10^7), DIF-12 (2.0×10^7), cyc⁻ (4.0×10^7), Φ2 (2.0×10^7), or MDCK cells (2.0×10^7) stably expressing αs-WT or αs-AVDT, derived from 40-ml culture volumes, were fractionated and HA-tagged αs proteins were then detected by immunoblotting with the monoclonal antibody 12CA5 after immunoprecipitation with the same antibody, as described in *Materials and Methods*. (*B*) cAMP accumulation in cells stably expressing αs-WT or αs-AVDT. cAMP accumulation of the stable cells expressing αs-WT or αs-AVDT described in *A* was assayed as described in *Materials and Methods*. Briefly, cells were seeded in 24-well plates at 1.5×10^5 (cyc⁻ cells) or at 0.75×10^5 (other cells) cells per well and labeled with [³H]adenine (4 μCi/ml, Amersham Pharmacia) for an additional 16 h. Cells were then washed once with DMEM and incubated in the presence of 3-isobutyl-1-methylxanthine (IBMX) for 30 min. cAMP and ATP fractions were resolved, and cAMP accumulation was estimated by the radioactivity of cAMP and ATP. Values represent means ± SD of triplicate determinations. (*C*) Localization of recombinant αs proteins in IEC-6 cells and cyc⁻ cells stably expressing αs-R201C. The cells were fractionated, and HA-tagged αs proteins were detected by immunoblotting with 12CA5 after immunoprecipitation with that same antibody. Each set of results is representative of at least two additional experiments. Sup, supernatant.

mutant is extremely unstable in the presence of GTP (Fig. 2*E*). We found that αs-AVDT activates adenylyl cyclase normally in the presence of GTP[γS] (Fig. 2*C*) and interacts with βγ, as assessed by the inhibition of the apparent on rate of GTP[γS] binding to αs-AVDT via βγ (data not shown).

From these biochemical analyses, we conclude that αs-AVDT is constitutively active but also unstable.

The Loss of Function of αs-AVDT Underlies the Associated Onset of PHP-Ia. We confirmed the constitutive activity and instability of αs-AVDT in intact cells by first stably expressing αs-WT and αs-AVDT in cyc⁻ cells, which lack endogenous αs, and then analyzing the cAMP accumulation both in the resting state and after receptor stimulation (Fig. 3). In the resting state, cyc⁻ clones expressing αs-AVDT showed marginal levels of constitutive activity. After β2 adrenergic receptor stimulation, the cAMP levels in the cyc⁻ clones expressing αs-WT increased, but in those expressing αs-AVDT these levels decreased (Fig. 3), suggesting that αs-AVDT is a loss-of-function mutant particularly in the presence of receptor stimulation. Incubation of these cells with pertussis toxin did not reverse this receptor-dependent inhibition (Fig. 3*B*), thus excluding the alternative possibility that the activation of G_i/G_o was involved. The expression levels of αs-AVDT were far lower than those of αs-WT in every clone (as indicated by the immunoblot shown in Fig. 3*A Lower*), which was in agreement with our biochemical data indicating that αs-AVDT is unstable in the presence of GTP. Hence, the instability and paradoxical inactivation by receptor stimulation results in a loss of function for the αs-AVDT mutant, which likely explains the resulting PHP-Ia phenotype.

The Cell-Specific Localization and Palmitoylation of αs-AVDT May Explain the Associated Neonatal Diarrhea. Intriguingly, the familial αs-AVDT mutation is associated with neonatal diarrhea in addition to PHP-Ia. We speculated that the enhanced constitutive activity of αs-AVDT in intestinal cells may be the underlying cause of this association, in a similar manner to cholera toxin (19). If this were indeed the case, we could then postulate at least two (although not necessarily mutually exclusive) possible mechanisms. One mechanism would be that the expression of αs-AVDT is increased in intestinal epithelial cells because of some stabilization mechanism. The other would be that αs-AVDT is specifically localized in the membrane where adenylyl cyclase is also present. We favor this latter possibility as the more likely of the two and thus analyzed the forced expression and localization of αs-WT and αs-AVDT in various cell lines, including IEC-6 and DIF-12 cells derived from the epithelia of rat and mouse small intestine, respectively.

We first examined the total expression levels of αs-AVDT in various cell types and found few differences among them. We then assessed the localization of αs (Fig. 4*A*) and found that αs-WT, inactive in the resting state, was recovered in membrane fractions from all of the cell types tested, which is consistent with

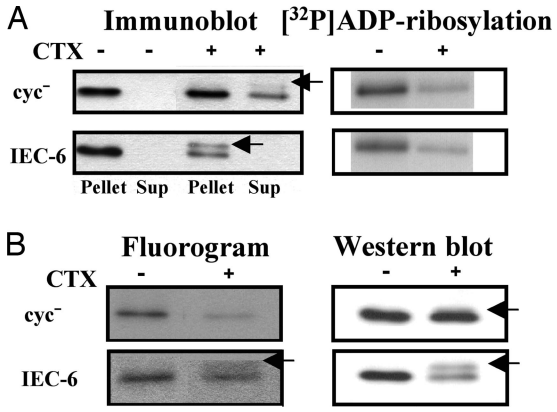

Fig. 5. Effects of activation by cholera toxin (CTX) on the localization (*A*) and palmitoylation (*B*) of recombinant αs proteins in cyc⁻ or IEC-6 cells expressing HA-tagged αs-WT. (*A*) cyc⁻ (1.0×10^7) or IEC-6 (0.5×10^7) cells derived from 10-ml culture volumes were fractionated, and HA-tagged αs proteins were detected by immunoblotting with monoclonal antibody 12CA5 after immunoprecipitation with the same antibody. Membrane fractions of these cells were also prepared in which the αs was [^{32}P]ADP-ribosylated with a 50 μg/ml concentration of activated cholera toxin. [^{32}P]ADP-ribosylated HA-tagged αs proteins were then visualized by autoradiography after immunoprecipitation as described in *Materials and Methods*. Before fractionation, the cells were incubated without or with 1 μg/ml cholera toxin for 4 h. (*B*) cyc⁻ (5.0×10^7) or IEC-6 (2.5×10^7) cells derived from 50-ml culture volumes were incubated for 2 h in DMEM containing 10% dialyzed FBS, 5 mM sodium pyruvate, and 0.5 mCi/ml [9,10-^{3}H]palmitic acid. After labeling, the cells were incubated without or with cholera toxin for 4 h and fractionated. Palmitoylated HA-tagged αs proteins were visualized by fluorography (30-day exposure), and HA-tagged αs proteins were detected by immunoblotting after immunoprecipitation as described in *Materials and Methods*. Arrows indicate αs proteins that have been ADP-ribosylated by cholera toxin. Each set of results is representative of at least two additional experiments.

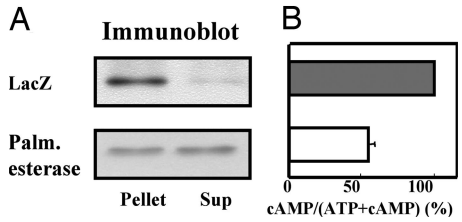

Fig. 6. Effects of APT1 or LacZ adenovirus infection on the localization of HA-tagged αs-AVDT (*A*) and on the accumulation of cAMP (*B*) in IEC-6 cells expressing HA-tagged αs-AVDT. (*A*) IEC-6 cells stably expressing αs-AVDT derived from a 40-ml culture volume were infected by recombinant APT1 adenovirus or LacZ adenovirus (at a multiplicity of infection of 50). After 48 h, the cells were fractionated, and HA-tagged αs-AVDT was detected by immunoblotting with the 12CA5 antibody. Each set of results is representative of at least two additional experiments. Palm. esterase, palmitoyl esterase; Sup, supernatant. (*B*) cAMP accumulation in stable cells in *A* was assayed as described in *Materials and Methods*. Values represent the means ± SE of three independent experiments with triplicate determinations.

the findings of previous reports (20, 21). In contrast, αs-AVDT, which is constitutively active in the resting state, was found to be predominantly localized in the membranes of the IEC-6 and DIF-12 cells but in the cytosol of several of the other cell types tested (cyc⁻ cells, Φ2 fibroblasts, and also MDCK cells that were derived from renal epithelial cells involved in the PHP-Ia phenotype). Moreover, the cAMP levels in the cell types stably expressing αs-AVDT tended to correlate with the αs-AVDT membrane expression levels (Fig. 4*B*). We speculated that the emergence of this phenotype is not limited to αs-AVDT but is in fact common among constitutively active αs mutants. Consistent with this, αs-R201C, another constitutively active αs mutant, also was found to be predominantly localized in the membranes of IEC-6 cells (Fig. 4*C*) but in the cytosol of cyc⁻ cells (20).

As a further experiment, we used cholera toxin to assess the activation-dependent translocation of αs. When αs-WT was activated by cholera toxin-induced ADP ribosylation (arrows in Fig. 5*A*), it did not translocate to the cytosol in IEC-6 cells stably expressing αs-WT but did so in cyc⁻ cells (Fig. 5*A Left*). We speculated that ≈70% of the αs-WT proteins were ADP-ribosylated in both cell types, as assessed by the cholera toxin-induced [^{32}P]ADP ribosylation of αs-WT that had not been ADP-ribosylated in the cells after 4 h of incubation with cholera toxin (Fig. 5*A Right*).

An important question that emerged from our current data is why the αs-AVDT mutant, which is active in the resting state, localizes at the membrane in intestinal epithelial cells. We and others have previously demonstrated that the localization and activity of αs are regulated by the palmitoylation/depalmitoylation cycle (22–24). Moreover, at rest, αs is anchored at the membranes by two mechanisms, interaction with $G_{\beta\gamma}$ and palmitoylation. When activated by receptor stimulation or other stimuli, αs is released from $G_{\beta\gamma}$ and depalmitoylated by palmitoyl esterase, leading to its translocation from the membrane to the cytosol. The activation-dependent translocation of αs has been observed in some studies (20, 24–28) but has been unsubstantiated in another study (29), suggesting that this translocation may be regulated by a cell-specific mechanism.

We thus hypothesized that one possible reason that both αs-AVDT and activated αs-WT localize at the membrane in IEC-6 cells is because depalmitoylation is inhibited in these cells. In support of this, our present data show that, after activation by cholera toxin, αs-WT harbors palmitate in IEC-6 cells (arrow in Fig. 5*B Left*) but not in cyc⁻ cells (Fig. 5*B*). The incorporated radioactivity (Fig. 5*B*) was shown to be linked to αs-WT by a thioester linkage, because it was removed by incubation with hydroxylamine (data not shown). Moreover, Western blots of the total αs protein levels in parallel samples ruled out the alternative possibility that the decrease of palmitoylation simply reflects a decrease of protein expression (Fig. 5*B Right*).

Given that the palmitoylation/depalmitoylation cycle may indeed involved in αs localization, we speculated that αs-AVDT may translocate from the membrane to the cytosol in IEC-6 cells when a palmitoyl esterase (see also *Discussion*) was overexpressed. To test this, we introduced acyl-protein thioesterase 1 (APT1) (30) cDNA or LacZ cDNA into IEC-6 cells stably expressing αs-AVDT by adenovirus-mediated gene delivery. We subsequently found that, when APT1 is overexpressed, ≈50% of the exogenous αs-AVDT is indeed translocated from the membrane to the cytosol (Fig. 6*A*) and that cAMP accumulation in the resting state is concomitantly reduced (Fig. 6*B*). These results suggest that, even in IEC-6 cells, αs-AVDT can translocate to the cytosol if it is depalmitoylated.

Significantly, our current findings suggest that the unique neonatal diarrhea phenotype associated with the familial αs-AVDT genotype may be caused by the enhanced constitutive activity of αs-AVDT in intestinal cells.

Discussion

Here we have elucidated that the principal molecular mechanism underlying a unique syndrome, PHP-Ia/neonatal diarrhea, is likely to be mediated via αs-AVDT. We speculated that PHP-Ia in this instance results from the instability and paradoxical receptor-dependent inactivation of αs-AVDT and also that associated neonatal diarrhea may result from the enhanced constitutive activity of αs-AVDT in the intestine.

We discuss in detail below why the αs-AVDT is a loss-of-function mutant that leads to the onset of PHP-Ia and why this

mutant may also cause neonatal diarrhea. Furthermore, we discuss the potential role of palmitoylation in determining the activity and localization of $G_{s\alpha}$ in a cell-specific manner.

The Mechanisms Underlying the Loss of Function of αs-AVDT. The loss of function of αs-AVDT seems to result from a combination of two mechanisms. First, a rapid GDP release from αs-AVDT results in its constitutive activity but also destabilizes the protein. We and others have reported in this regard that αs in its guanine nucleotide-free form denatures more rapidly than in its GDP/GTP binding form (12, 31). The instability of αs-AVDT may thus be due to a rapid denaturation from a guanine nucleotide-free form of this protein, at least in part. In support of this, our current data show that although αs-AVDT is stable once it binds GTP[γS], it is very unstable in the presence of GTP (Fig. 2*E*).

Second, αs-AVDT can be additionally characterized by the fact that receptor stimulation does not potentiate but in fact inhibits its constitutive activity. This phenomenon may be explained by the fact that receptor stimulation has been shown to confer a decreased affinity for G_α for both GTP and GDP (5, 14, 32). The mutant αs-AVDT protein itself has a low affinity for guanine nucleotides, and, when this is further decreased by receptor stimulation, its ability to bind guanine nucleotides may be lost (5), and its constitutive activity may thus be impaired.

The Onset of Neonatal Diarrhea Resulting from the αs-AVDT Mutation. One of the most common mechanisms underlying the cause of diarrhea is the irreversible activation of $G_{s\alpha}$ by the toxin produced by *Vibrio cholerae*, which ADP-ribosylates an arginine residue in the switch II region of this G protein. In small intestinal cells, cAMP activates protein kinase A and thus induces protein phosphorylation, which increases Cl secretion and inhibits NaCl-coupled absorption (19). If αs-AVDT is localized at the membrane in intestinal cells, its constitutive activity may be enhanced, resulting in excess signaling over threshold even when the protein is expressed at very low levels. Hence, cAMP may accumulate in intestinal cells and cause diarrhea.

We further speculated as to why the symptoms of diarrhea caused by αs-AVDT were observed only during the neonatal period. This could be explained by adaptation mechanisms that activate only at a later stage because the increased basal levels of cAMP are in general very toxic to the cells (1, 33). One such mechanism may be the up-regulation of palmitoyl esterase. Alternatively, the constitutive activity of αs-AVDT may be attenuated by the development of G_s protein-coupled receptor signaling because, as shown above, receptor stimulation somewhat paradoxically inhibits the constitutive activity of αs-AVDT.

Palmitoylation May Regulate the Cell-Specific Activity and Localization of $G_{s\alpha}$. The regulation of receptor localization and activity is one of the most common mechanisms that desensitize the cell in the face of persistent stimulation. Second messenger-regulated kinases, G protein-coupled receptor kinases, and the arrestins play central roles in this process (34). In addition, regulatory mechanisms at the level of G proteins may exist, as has previously been reported (22, 23, 28, 29, 35, 36).

A dynamic and reversible modification by palmitoylation is thought to control the activity and localization of $G_{s\alpha}$, $G_{q\alpha}$, endothelial nitric oxide synthase (eNOS), and many other signaling molecules (37). $G_{s\alpha}$ attaches to the plasma membrane via two mechanisms: palmitate and its interaction with $G_{\beta\gamma}$. Palmitoylation is dynamically regulated (22), and the activation of $G_{s\alpha}$ by receptor or other stimuli accelerates depalmitoylation/palmitoylation turnover and translocation. We and others have proposed working models showing that activation causes accelerated depalmitoylation, leading to the translocation of $G_{s\alpha}$ to the cytosol. One simple possibility that can be derived from this hypothesis is that, when activated and dissociated from $G_{\beta\gamma}$, $G_{s\alpha}$ becomes more susceptible to palmitoyl esterase: it has been shown that the binding of $G_{\beta\gamma}$ protects $G_{s\alpha}$ from attack by such esterases (22, 23).

The specific enzyme responsible for the depalmitoylation of $G_{s\alpha}$ has not yet been identified in any cell type (38). However, APT1 can cleave palmitate from $G_{s\alpha}$ or ras proteins *in vitro* (30). In yeast, APT is more specific for the G protein α subunit, Gpa1p, compared with ras (39). In addition, a knockout of the APT1 gene in yeast impairs yeast G_α protein (Gpa1p)-associated thioacyl group turnover. However, APT1 does not remove palmitate from all proteins, indicating that other enzymes must be required to fulfill this role even in yeast. Another enzyme, palmitoyl protein thioesterase 1, was found to be responsible for lysosomal protein degradation (36, 38).

Our findings here indicate that the activation of $G_{s\alpha}$ causes its depalmitoylation, which in turn causes a translocation of this protein from the plasma membrane to the cytosol and a dampening of the signal. Several lines of evidence support this contention. (*i*) In small intestinal cells (IEC-6 and DIF-12 cells), activated $G_{s\alpha}$ is predominantly localized at the membrane, but in other cell types tested it accumulates mostly in the cytosol. (*ii*) αs-AVDT is a constitutively active $G_{s\alpha}$ and seems to activate adenylyl cyclase more strongly in IEC-6 and DIF-12 cells than in several other cells tested. (*iii*) In IEC-6 cells, the activation of αs (by cholera toxin) does not seem to decrease the degree of palmitoylation of $G_{s\alpha}$, although it does so in cyc^- and other cells (21, 22). (*iv*) The overexpression of APT1 reverses, at least in part, the membrane localization and the constitutive activity of αs-AVDT.

The results of this study thus not only support the notion that the palmitoylation cycle regulates the localization and activity of $G_{s\alpha}$ but also suggests that this may occur in a cell-specific manner. The interesting question of whether depalmitoylation may possibly be another example of a signal-desensitization mechanism working at the G protein level remains to be addressed. However, if this notion proves to be correct, the palmitoylation cycle itself would become a desirable target for the development of novel treatments against human diseases resulting from abnormal signal desensitization, including chronic heart failure (40, 41) and hypertension (1, 42, 43).

Conclusions

The αs-AVDT familial mutation causes PHP-Ia because of instability and paradoxical inactivation by receptor stimulation. The associated neonatal diarrhea that occurs may be caused by the constitutive activity of αs-AVDT, which is possibly enhanced by the membrane localization of this protein in intestinal cells. Moreover, our present study suggests that palmitoylation may regulate the activity and localization of $G_{s\alpha}$ in a cell-specific manner.

Materials and Methods

Purification of αs Proteins. Recombinant αs-WT and αs-AVDT were purified from the cytosol of Sf9 cells infected with baculovirus encoding the corresponding αs protein constructs (14). Sf9 cells (1.5×10^6 cells per ml) were maintained in Sf-900 II medium (Invitrogen, Carlsbad, CA) at 27.5°C and infected with the baculoviruses at a concentration of three plaque-forming units per cell. After cell lysis by using nitrogen cavitation, the supernatant fractions were sequentially chromatographed on columns of HiTrap Q (Amersham Pharmacia, Uppsala, Sweden; 5-ml bed volume × 2) (12), Econo-Pac (Bio-Rad, Hercules, CA; 5-ml bed volume) with a potassium phosphate gradient (44), and Resource Q (GE Healthcare, Piscataway, NJ; 1-ml bed volume) (45) in the absence of detergents.

GTP[γS] Binding and GTPase Assays. GTP[γS] binding and GTP hydrolysis were quantitated as described previously (12, 45). The apparent on rates (k_{app}) of GTP[γS] binding and the rate constants for a single turnover of GTP hydrolysis were quantitated also as earlier described (44, 45).

cAMP Assay. cAMP accumulation in intact S49 cyc$^-$ cells (12, 46) and cAMP synthesis by recombinant αs in membranes of the same cells (12, 47) were assayed as described previously. Before performing the latter assay, the αs proteins were incubated with 100 μM guanine nucleotide for 30 min (WT) or 1 min (mutant).

Cell Culture and Transfection. S49 cyc$^-$ cells, maintained in DMEM containing 10% (vol/vol) horse serum, were transfected with a retroviral pMV7 construct encoding HA-tagged αs-WT or αs-AVDT, and stable clones were selected as described previously (12, 14, 20). Rat intestinal epithelial cells (IEC-6 cells) (48), Φ2 fibroblasts (20), and MDCK cells (purchased from the American Type Culture Collection, Manassas, VA) were maintained in DMEM containing 5–10% (vol/vol) FBS and were transfected in the same manner as S49 cyc$^-$ cells. Stable clones in these cases were selected by using 0.4–1.0 mg/ml G418 in the growth medium. Membrane fractions of S49 cyc$^-$ cells were prepared after nitrogen cavitation as described earlier (12, 49). HEK 293 cells (50) were cotransfected by calcium phosphate precipitation to obtain the desired recombinant adenoviruses, as described previously (51). DIF-12 duodenal epithelial cell lines were established from *p53*$^{-/-}$ fetal mice (H.F. and Y.Y., unpublished data) by using techniques similar to those used for establishing gastric epithelial cell lines (52). As has been reported for gastric epithelial cell lines (53), DIF-12 cells exhibited polarity with occasional glandular structures in organ culture (data not shown).

Palmitate Labeling. S49 cyc$^-$ cells or IEC-6 cells expressing HA-tagged αs-WT were incubated for 2 h in DMEM containing 10% dialyzed serum and 0.5 mCi/ml [9,10-^{3}H]palmitic acid (1 Ci = 37 GBq) as described previously (22).

Cell Fractionation. For the analysis of the subcellular distribution of αs, the cells were homogenized with a Dounce homogenizer, and the supernatant fraction (cytosol fraction) and the pellet (membrane fraction) were prepared as described previously (21, 22).

Immunoprecipitation, Western Blotting, and ADP Ribosylation. HA-tagged αs proteins were immunoprecipitated by using the 12CA5 monoclonal antibody as described earlier (12, 20). Western blotting and fluorography were performed as described previously (22, 23). [^{32}P]ADP ribosylation of αs by cholera toxin was performed as described (49).

We thank J. A. Duncan (University of North Carolina, Chapel Hill, NC) and A. G. Gilman (University of Texas Southwestern Medical Center, Dallas, TX) for generously donating the APT1 construct. We also thank H. R. Bourne for helpful suggestions. This work was supported by a Grant-in-Aid for Scientific Research and Research on Priority Area from the Ministry of Education, Science, Sports, and Culture of Japan (to T.I.).

1. Farfel Z, Bourne HR, Iiri T (1999) *N Engl J Med* 340:1012–1020.
2. Spiegel AM, Weinstein LS (2004) *Annu Rev Med* 55:27–39.
3. Aldred MA (2006) *J Pediatr Endocrinol Metab* 19:S635–S640.
4. Lania AG, Mantovani G, Spada A (2006) *Nat Clin Pract Endocrinol Metab* 2:681–693.
5. Iiri T, Farfel Z, Bourne HR (1998) *Nature* 394:35–38.
6. Bourne HR, Sanders DA, McCormick F (1991) *Nature* 349:117–127.
7. Gilman AG (1995) *Biosci Rep* 15:65–97.
8. Cabrera-Vera TM, Vanhauwe J, Thomas TO, Medkova M, Preininger A, Mazzoni MR, Hamm HE (2003) *Endocr Rev* 24:765–781.
9. Schwindinger WF, Miric A, Zimmerman D, Levine MA (1994) *J Biol Chem* 269:25387–25391.
10. Linglart A, Carel JC, Garabédian M, Lé T, Mallet E, Kottler ML (2002) *J Clin Endocrinol Metab* 87:189–197.
11. Linglart A, Mahon MJ, Kerachian MA, Berlach DM, Hendy GN, Juppner H, Bastepe M (2006) *Endocrinology* 147:2253–2262.
12. Iiri T, Herzmark P, Nakamoto JM, Van Dop C, Bourne HR (1994) *Nature* 371:164–168.
13. Farfel Z, Iiri T, Shapira H, Roitman Z, Mouallem M, Bourne HR (1996) *J Biol Chem* 271:19653–19655.
14. Iiri T, Farfel Z, Bourne HR (1997) *Proc Natl Acad Sci USA* 94:5656–5661.
15. Warner DR, Gejman PV, Collins RM, Weinstein LS (1997) *Mol Endocrinol* 11:1718–1727.
16. Warner DR, Weng G, Yu S, Matalon R, Weinstein LS (1998) *J Biol Chem* 273:23976–23983.
17. Aldred MA, Bagshaw RJ, Macdermot K, Casson D, Murch SH, Walker-Smith JA, Trembath RC (2000) *J Med Genet*, 37:E35.
18. Higashijima T, Ferguson KM, Smigel MD, Gilman AG (1987) *J Biol Chem* 262:757–761.
19. Kaper JB, Morris JG, Jr, Levine MM (1995) *Clin Microbiol Rev* 8:48–86.
20. Levis MJ, Bourne HR (1992) *J Cell Biol* 119:1297–1307.
21. Wedegaertner PB, Chu DH, Wilson PT, Levis MJ, Bourne HR (1993) *J Biol Chem* 268:25001–25008.
22. Wedegaertner PB, Bourne HR (1994) *Cell* 77:1063–1070.
23. Iiri T, Backlund PB, Jones TLZ, Wedegaertner PB, Bourne HR (1996) *Proc Natl Acad Sci USA* 93:14592–14597.
24. Wedegaertner PB, Bourne HR, von Zastrow M (1996) *Mol Biol Cell* 7:1225–1233.
25. Ransnas LA, Svoboda P, Jasper JR, Insel PA (1989) *Proc Natl Acad Sci USA* 86:7900–7903.
26. Yu JZ, Rasenick MM (2002) *Mol Pharmacol* 61:352–359.
27. Hynes TR, Mervine SM, Yost EA, Sabo JL, Berlot CH (2004) *J Biol Chem* 279:44101–44112.
28. Marrari Y, Crouthamel M, Irannejad R, Wedegaertner PB (2007) *Biochemistry* 46:7665–7677.
29. Mumby SM (1997) *Curr Opin Cell Biol* 9:148–154.
30. Duncan JA, Gilman AG (1998) *J Biol Chem* 273:15830–15837.
31. Higashijima T, Ferguson KM, Sternweis PC, Smigel MD, Gilman AG (1987) *J Biol Chem* 262:762–766.
32. Berstein G, Blank JL, Smrcka AV, Higashijima T, Sternweis PC, Exton JH, Ross EM (1992) *J Biol Chem* 267:8081–8088.
33. Happle R (1986) *Clin Genet* 29:321–324.
34. Lefkowitz RJ (2004) *Trends Pharmacol Sci* 25:413–422.
35. Chen CA, Manning DR (2001) *Oncogene* 20:1643–1652.
36. Linder ME, Deschenes RJ (2007) *Nat Rev Mol Cell Biol* 8:74–84.
37. Smotrys JE, Linder ME (2004) *Annu Rev Biochem* 73:559–587.
38. Lu JY, Hofmann SL (2006) *J Lipid Res* 47:1352–1357.
39. Duncan JA, Gilman AG (2002) *J Biol Chem* 277:31740–31752.
40. Rockman HA, Koch WJ, Lefkowitz RJ (2002) *Nature* 415:206–212.
41. Riddle EL, Schwartzman RA, Bond M, Insel PA (2005) *Circ Res* 96:401–411.
42. Métayé T, Gibelin H, Perdrisot R, Kraimps JL (2005) *Cell Signalling* 17:917–928.
43. Felder RA, Jose PA (2006) *Nat Clin Pract Nephrol* 2:637–650.
44. Graziano MP, Gilman AG (1989) *J Biol Chem* 264:15475–15482.
45. Iiri T, Ohaka Y, Ui M, Katada T (1992) *J Biol Chem* 267:1020–1026.
46. Iiri T, Bell SM, Baranski TJ, Fujita T, Bourne HR (1999) *Proc Natl Acad Sci USA* 96:499–504.
47. Markby DW, Onrust R, Bourne HR (1993) *Science* 262:1895–1901.
48. Quaroni A, Wands J, Trelstad RL, Isselbacher KJ (1979) *J Cell Biol* 80:248–265.
49. Iiri T, Tohkin M, Morishima N, Ohoka Y, Ui M, Katada T (1989) *J Biol Chem* 264:21394–21400.
50. Makita N, Sato J, Manaka K, Shoji Y, Oishi A, Hashimoto M, Fujita T, Iiri T (2007) *Proc Natl Acad Sci USA* 104:5443–5448.
51. Miyake S, Makimura M, Kanegae Y, Harada S, Sato Y, Takamori K, Tokuda C, Saito I (1996) *Proc Natl Acad Sci USA* 93:1320–1324.
52. Li QL, Ito K, Sakakura C, Fukamachi H, Inoue K, Chi XZ, Lee KY, Nomura S, Lee CW, Han SB, *et al.* (2002) *Cell* 109:113–124.
53. Fukamachi H, Ito K, Ito Y (2004) *Biochem Biophys Res Commun* 321:58–64.